Environmental
Science
Processes & Impacts

ROYAL SOCIETY
OF CHEMISTRY

Charge-Assisted Hydrogen Bonding as a Cohesive Force in Soil Organic Matter: Water Solubility Enhancement by Addition of Simple Carboxylic Acids

SCHOLARONE™
Manuscripts

Environmental Significance Statement

Cohesive forces within natural organic matter (OM) play crucial roles in the biogeochemical behavior of OM and its interactions with pollutants, but are not well understood. This study shows that weak acids, but not other hydrogen (H)-bonding solutes, increase the water solubility of OM in a reference soil. The pattern is consistent with the disruption of (negative) charge-assisted H bonds between carboxyl groups on OM segments or separate molecules, and formation of new ones with the solute, as a main cause. The (-)CAHB is an extraordinarily strong type of H bond between groups of similar proton affinity, or pK_a. Besides solubility, the results are potentially broadly significant for OM adsorption, aggregation in solution, metal ion complexation, and bonding with chemicals and engineered nanoparticles.

1　Charge-Assisted Hydrogen Bonding as a Cohesive Force in Soil Organic Matter:

2　Water Solubility Enhancement by Addition of Simple Carboxylic Acids

3　Jinzhi Ni[a,b] and Joseph J. Pignatello[a]*

4

5　[a]Department of Environmental Sciences, The Connecticut Agricultural Experiment Station, 123

6　Huntington St., New Haven, Connecticut, 06504-1106, U.S.A.

7　[b]Permanent address: College of Geographical Sciences, Fujian Normal University, Fuzhou 350007 China

8　*Corresponding author: joseph.pignatello@ct.gov; +1(203) 974-8518

9

10   **Abstract:**

11   Weak bonds between molecular segments and between separate molecules of natural organic

12   matter (OM) govern its solubility, adsorption, supramolecular association in solution, and complexation

13   with metal ions and oxides. We tested the hypothesis that especially strong hydrogen bonds, known as

14   (negative) charge-assisted hydrogen bonds, (-)CAHB, contribute significantly to OM cohesion and

15   increase water solubility of solid-phase OM. The (-)CAHB, exemplified by structures such as

16    $(-CO_2 \cdots H \cdots O_2C-)^-$ and $(-CO_2 \cdots H \cdots O-)^-$, may form between weak acids with similar proton affinity, and

17   is shorter, more covalent, and much stronger than ordinary hydrogen bonds. Using a high-organic

18   reference soil, we show that (-)CAHBs within the solid OM phase (intra-OM) are disrupted by solutions

19   of aliphatic and aromatic acids, resulting in enhanced solubility of OM. The aromatic acids included

20   naturally occurring plant exudate compounds. At constant pH and ionic strength, OM solubility increased

21   with added organic acid concentration and molecular weight. Polar compounds incapable of forming

22   (-)CAHBs, such as alkanols, acetonitrile, and dimethyl sulfoxide, were ineffective. Solubility

23   enhancement showed behavior consistent with (-)CAHB theory and published observations—namely, *i*)

24   that formate is more effective than acetate due to its tendency to form stronger (-)CAHBs; *ii*) that

25   solubility enhancement peaks at pH ~5-6, where the product of interacting carboxylate ion concentrations

26   reaches a maximum; and *iii*) that elution of acetate or formate through soil columns releases hydroxide

27   ion, consistent with formation of (-)CAHBs between added acid and free weak acid groups on the solid

28   OM. The results support the hypothesis that the (-)CAHB contributes to the cohesion of OM in the solid

29   state.

30   **Keywords:** Pahokee Peat; hydrogen bond; soil organic matter; humic substances; low-barrier hydrogen

31   bond; charge-assisted hydrogen bond; plant exudate;

1. INTRODUCTION

Natural organic matter (OM) plays important roles in microbial activity, soil structure, mineral weathering, nutrient availability to plants, carbon storage, and pollutant fate. Establishing the biogeochemical roles of OM requires a molecular level understanding of the interactions of OM molecules with each other and with mineral and biological surfaces. Coming to such understanding has been challenging due to the intrinsic heterogeneity of OM on the microscopic, macroscopic, and geographic scales. The historical conceptual model of dissolved OM regards it as a macromolecular substance composed of individual molecules that randomly coil in solution as a result of weak forces and the hydrophobic effect, and that uncoil as pH rises due to charge repulsion between segments. The macromolecular model is based on molecular weight distribution derived from sedimentation velocity [1, 2] and other observations [3, 4]. Recently, a supramolecular model was proposed that regards DOM as a self-assembled association of relatively small molecules that bind intermolecularly by weak forces and the hydrophobic effect. This concept is supported by a shift to lower molecular weight (size exclusion chromatography) or greater translational diffusion coefficients (nuclear magnetic resonance) after decreasing the DOM concentration or adding organic solutes [5-12]. In addition, molecular weights as low as ~200 g/mole have been observed in high resolution mass spectra of some DOM samples [13]. Solid phase OM (SOM) is also regarded as a supramolecular aggregate, but on a grander scale. The partitioning of OM between the solid and liquid phases (i.e., its solubility) is governed in part by interactions within the solid OM phase ("intra-OM", including intermolecular and intramolecular interactions) because OM can exist as discrete particles or as multilayer patches on mineral surfaces in soil and sediments.

Regardless of the conceptual model of OM, an underlying issue of importance is the nature of the forces holding molecular segments and separate molecules together. Participation of van der Waals (dispersion, induction, dipolar), metal ion bridging, and hydrogen (H) bonding have been widely invoked [9-11, 14]. While van der Waals forces can be taken for granted, and while computations have lent insight into metal ion involvement and H-bonding [15, 16], there is surprisingly little experimental data backing the

57 existence and contributions of these interactions to the cohesive forces of OM. The present study

58 addresses H-bonding. The breakup of supramolecular aggregates of DOM to smaller, faster-diffusing

59 molecules upon addition of methanol, acetic acid, or propionic acid was attributed to disruption of van der

60 Waals, π-π, and CH-π forces [9, 10] or H-bonding forces [12]. The reduction in average molecular weight of

61 dissolved Suwannee River Fulvic Acid (by electrospray ionization-mass spectrometry) after methylation

62 with diazomethane was taken as evidence for disaggregation caused by disruption of intra-OM H-bonding

63 involving carboxyl groups [14]. Ordinary intra-OM H-bonds face strong competition from water molecules

64 [17]. Molecular dynamics simulations of hypothetical humic molecules show that, as hydration increases,

65 OM-OM H-bonds decrease in abundance [16], leveling off after a point [15], whereas OM-water H-bonds

66 increase in abundance [15].

67   A potential contribution to OM cohesion that has so far been overlooked is the exceptionally-strong

68 H-bond that can form between a favorably-orientated donor-acceptor pair having closely-similar proton

69 affinity (or pK_a), known as the Charge-Assisted Hydrogen Bond (CAHB). Of particular relevance is the

70 negative (-) CAHB formed by conjugate pairs of carboxylate, phenolate, or enolate groups, which are

71 abundant in OM. These bonds may be written $(-CO_2\cdots H\cdots O_2C-)^-$, $(-CO_2\cdots H\cdots O-)^-$, or $(-O\cdots H\cdots O-)^-$.

72 Also known are (+/-)CAHB and (+)CAHB formed by conjugation of N/O and N/N donor-acceptors with

73 closely-similar pK_a, but weak acid N groups are much less abundant in OM. The CAHB is a subset of the

74 Low Barrier Hydrogen Bond (LBHB), so-called because the energy barrier for proton exchange between

75 heteroatoms is small or zero, creating a bond that is shorter, more covalent, and much stronger than

76 ordinary H bonds [18, 19]. The strength of the LBHB increases as the difference in acidity constants of the

77 donor and acceptor groups, ΔpK_a, approaches zero [19-21]. The (-)CAHB owes its exceptional strength to the

78 close sharing of the proton due to the small ΔpK_a and the participation of the negative charge in

79 stabilization of the complexed proton. The sterically-unhindered (-)CAHB between carboxyl groups is the

80 strongest H-bond known among organic compounds [18, 20-23]. Homoconjugation of phenols and

81 heteroconjugation between a phenol and carboxylic acid are somewhat weaker. The CAHB are believed

4

82   to be involved in intermediate or transition state stabilization of enzymatic reactions [24] and in the structure

83   of metal-organic and inorganic molecular networks [25, 26]. Recent studies show that the (-)CAHB is

84   important in adsorption of weak acids, including carboxylic acids, sulfonamides, and phenols to

85   carbonaceous materials such as chars and partially-oxidized carbon nanotubes, whose surfaces are

86   abundant in carboxyl/phenoxyl groups [27 17, 28-30].

87   We proposed that exceptionally strong intramolecular and intermolecular (-)CAHBs can be counted

88   among the important cohesive forces of SOM, and that disruption of such bonds can lead to greater

89   solubility of SOM. To test this hypothesis we examined solubility of SOM in a high-organic reference

90   soil after addition of simple aliphatic acids and single-ring aromatic acids and phenolic acids to the

91   aqueous phase. Many of the selected aromatic and phenolic acids have been identified in soils (e.g., [31]),

92   where they are released from living and decaying plants and can influence soil and humus formation,

93   metals complexation, mineral dissolution, allelopathy, nutrient bioavailability, and plant-microbe

94   interactions [32-35].

95   Certain features of the (-)CAHB are noteworthy in the context of the present study. First, unlike

96   ordinary H-bonds that form between non-ionizable groups with widely different pK_a values (e.g.,

97   alcohols, ethers, ketones, esters), the (-)CAHB is potentially strong enough to out-compete OM-water H-

98   bonds [17], especially within the OM phase, where the H_2O concentration is lower than in bulk solution.

99   Interestingly, molecular models of hydrated humic aggregates show that OM-OM H-bonds remain

100   constant at about 1 H-bond per 2 heteroatoms regardless of water content [15]. Second, maximum

101   conjugation occurs at a pH equal to the mean pK_a of the two reactants. The pK_a frequency in OM peaks

102   around 4-5 reflecting mainly carboxyl groups, and then again around 9-10 reflecting mainly phenolic

103   groups [36]. This means that OM cohesion due to (-)CAHB forces should maximize around pH 3-6 where

104   the carboxylate group dissociates, and then again around pH 8-10 where phenolic and other acidic

105   alcoholic groups dissociate. Third, water may supply a proton for the (-)CAHB, raising the bulk pH

106   according to the reaction:

107    $2A^- + H_2O \rightleftharpoons (A \cdots H \cdots A)^- + OH^-$ (1)

108   Our working hypotheses were as follows (Scheme 1). *a*) The organoanion solute can compete with

109   existing (-)CAHB between carboxyl groups on SOM to displace relatively water-soluble OM molecules,

110   leading to an increase in water solubility of SOM (Scheme 1a). The effectiveness of the organoanion may

111   depend on its molecular structure. *b*) The organoanions in solution can form new (-)CAHB with SOM by

112   abstracting a proton from water, resulting in the release of hydroxide (eq 1; Scheme 1b). The rise in bulk-

113   liquid pH associated with this reaction may be mitigated by the buffering capacity of the solid phase. *c*)

114   The organoanion solute can compete with existing intermolecular (-)CAHB between carboxyl groups on

115   separate DOM molecules to promote disaggregation in solution (Scheme 1c). Based on studies with a

116   high-organic reference soil we present data in support of (*a*) and (*b*) and defer consideration of (*c*) to a

117   later report.

118

2.   MATERIALS AND METHODS

119

2.1.   Materials

120

121   The source of SOM was the Pahokee (Florida) Peat Soil (BS103P) consisting of both humic and

122   fulvic acids purchased from the International Humic Substances Society. It contains 44.6 % C, 4.70 % H,

123   3.09 % N, and 6.9 % ash after combustion [37], and has a pH (1 g soil:2.5 mL H_2O) of 5.3. The carboxyl and

124   phenoxyl contents of fulvic and humic acids derived from this soil on the basis of titration curves have been

125   reported [36]. The organic aromatic acids and other reagents were purchased in the highest purity available.

126   Water was purified in a Milli-Q Integral 10 system.

127

2.2.   Batch solubility experiments

128

129   Pahokee Peat samples (0.20 g) along with 20 mL of organic acid solution (at pH 6.0) were placed in 20-

130   mL Teflon®-lined septum screw cap glass vials. Then, an amount of standard HCl or NaOH solution

131 determined according to preliminary experiment was added to each vial to attain a pH near 6. A control

132 was also made up containing only NaCl at the same molar concentration as organic acid; the ionic strength

133 of the control and samples was comparable since the dissolved organic acid was nearly completely

134 dissociated at pH 6. The vials were mixed end-over-end at 40 rpm at 20±1 ℃. At termination, the pH was

135 measured and the vials were centrifuged at 20°C and 1800 rpm for 40 min, and the supernatant (extract)

136 was filtered through a 0.45-μm PTFE membrane filter. Solubilization rate in 0.3 M p-hydroxylbenzoic acid

137 solution revealed that dissolution continues beyond 300 h, but slows down markedly after 24 h. Twenty

138 four hours was chosen as the operational solubility equilibration period for all systems.

2.3. Column elution experiments

140 These experiments employed a glass column (Benchmark, 150 mm×10 mm; Kinesis Inc.) equipped with

141 an adjustable Teflon plunger at each end. The column was packed with a mixture of Pahokee Peat and

142 glass microbeads (210-300μm, Sigma-Aldrich). The microbeads were pre-treated by soaking three times

143 in 0.1 M HCl for 24 h, washing repeatedly with water, and finally drying at 120 ℃. The column was

144 packed dry in a vertical position by layering a homogeneous mixture of Pahokee Peat (1 g) and

145 microbeads (6 g) between layers of microbeads alone at each end of the column (1 g at inlet and 2 g at

146 outlet), each layer being added all at once. The top plunger was inserted to eliminate free space and 2 M

147 NaCl solution adjusted to pH 5.3 was pumped through the column from the bottom up at a flow rate of

148 0.05 mL/min using a constant-volume HPLC pump (Agilent 1100). When the liquid began to elute from

149 the column, the flow was stopped and the column was allowed to condition for 14-16 h. Flow was

150 resumed at 0.2 mL/min until the pH of the effluent approached 5.3 and then the eluent was then changed

151 to 2 M organic acid solution that had been pre-adjusted to pH 5.3 and total ionic strength of 2 M with

152 NaCl; the amount of NaCl added was based on the calculated degree of dissociation of the organic acid

153 given its pK_a. Effluent was received to the bottom of a 1.0 mL vial in which a pH microprobe was

154 situated, and allowed to spill to waste. The pH was recorded approximately every 5 min. Approximately

155 every 10 min an aliquot of the effluent was collected from the same vial and passed through a 0.45 μm

156   PTFE filter prior to OM analysis. A diagram of the experiment is shown in Figure 1.

157

158   **2.4. Determination of DOM concentration**

159   Except for the controls, dissolved organic carbon (DOC) concentrations in the liquid samples

160   could not be determined with any precision by ordinary combustion analysis because the DOC levels

161   originating from the added organic solute were too high. Therefore, we used absorbance at 254 or 365 nm

162   as a surrogate for DOM concentration. The results are generally reported at 365 nm, but qualitatively

163   similar trends were obtained at both wavelengths in all experiments.

164   Figures 2a and 2b show that DOM absorbance of aqueous extracts or eluents of soil depends on

165   electrolyte (NaCl, Na-formate, or Na-acetate), electrolyte concentration, and pH. To eliminate these

166   effects in order to facilitate comparison among samples, the filtrate was pre-diluted in a phosphate buffer

167   (0.1 M; pH 6.5) by at least 10-fold and sufficient to keep the absorbance reading at 254 and 365 nm below

168   1. Figure 2c shows that, diluted in this way, absorbance over the entire spectrum from 250 – 500 nm

169   became independent of initial pH and electrolyte composition up to at least 2 M. The absorbance values

170   reported in all the figures apply to the calculated values for the original solutions.

171   To evaluate the correlation between absorbance and OC concentration, Pahokee Peat (0.2 g) was

172   mixed with 0.1 M NaCl (50 mL) and adjusted at different pH from 2 to 6 with NaOH or HCl using a

173   quantity determined in a preliminary experiment, and the samples. After end-over-end shaking at 20±1 ℃

174   for 24 h, the vials were centrifuged and the supernate filtered per the steps described above. Non-

175   purgeable total organic carbon (TOC) was measured in the filtrate by the high temperature combustion

176   method (Shimadzu TOC-500) against a potassium phthalate standard and compared with absorbance after

177   10-fold dilution into the pH-6.5 phosphate buffer, as above. The results (Figure 2d) show that A_{365} or A_{254}

178   correlates well with TOC. The non-zero intercept indicates a substantial concentration of DOC exists that

179   is colorless at these wavelengths, more so at 365 nm. Abouleish and Wells [38]observed a non-zero

180   intercept between A_{254} and DOC for various Pahokee peat and other fulvic and humic acid standards and

181 suggested that it was due to protein-like and carbohydrate-like components that do not absorb well at 254

182 nm.

183

3. RESULTS AND DISCUSSION

3.1. Studies in batch systems

186 Figure 3 shows the 24-h solubility of OM from Pahokee peat in 2 M solutions of formate, acetate,

187 methanol, or the NaCl-in-water control as a function of pH. All systems were adjusted with NaCl to the

188 same ionic strength at each pH, as depicted in the top graph. Solubility generally increased with pH, with

189 a steeper rise above pH ~7, as expected due to deprotonation of acidic groups. Features of these plots

190 support the (-)CAHB hypothesis. Addition of the (-)CAHB-capable organic acids greatly enhanced

191 solubility compared to methanol and the water control. Solubility is greater for formate than acetate,

192 consistent with the tendency of formate to form stronger (-)CAHB than acetate [39]. By contrast, solubility

193 is not enhanced—in fact, it is suppressed—by methanol. Methanol generally forms H bonds of only

194 ordinary strength at environmental pH. The H-bond between SOM acidic groups and methanol—e.g.,

195 $(-CO_2 \cdots HOCH_3)^-$ —are of the ordinary type because ΔpK_a is large (the pK_a of carboxyl groups is ~3-5,

196 and of methanol is 15.7). One could attribute solubility enhancement to a non-specific effect in which the

197 relatively apolar parts of the OM molecules are better solvated when an organic solute is present.

198 However, the lack of solubility enhancement for 2 M methanol suggests that a general solvophilic effect

199 cannot explain solubility enhancement by the organic acids. Lastly, solubility for formate and acetate

200 peaks around pH 5, which is near mean pK_a of the organic acid solute and the carboxyl groups of SOM.

201 As mentioned in the Introduction (Section 1), this corresponds to the most favorable pH for (-)CAHB

202 formation between interacting groups. Note that solubility in formate solution begins to peak at lower pH

203 values than in acetate solution, reflecting the lower pK_a value of formate (3.75 *vs* 4.76). The peak does not

204 appear in the water control or methanol systems, showing that ionic strength is not the cause. All of these

9

205   results are consistent with (-)CAHB formation between organic acids and acidic groups of SOM, allowing

206   greater solubility of SOM.

207   Figures 4a-4d shows the 24-h solubility of Pahokee peat SOM in solutions of different organic

208   acids or other polar organic solutes at pH ~6 where the organic acids are almost fully ionized. The solute

209   concentration in the panels varies to accommodate the different water solubilities of the organic acids.

210   Figures 4b - 4d show that SOM solubility in different organic acid solutions exceeds that of the control,

211   suggesting the involvement of (-)CAHB. In Figure 4a it can be seen that the solubility enhancement

212   observed for 1 M acetic acid is not observed for 1 M polar organic solutes that are incapable of forming

213   CAHBs because their pK_a values are too far-removed from those of the weakly acid groups on SOM;

214   these solutes include 2-propanol, dimethylsulfoxide, methanol, and acetonitrile. In fact, the solubility of

215   SOM in 1 M solutions of the polar solutes is actually *lower* than in the water control. The lack of

216   solubility enhancement for the polar co-solvents argues against a non-specific solvophilic-based

217   explanation for the solubility enhancement by the organic acids. The aromatic acids are more effective

218   than the two aliphatic acids tested. Note in Figure 4 the outlier, caffeic acid, which gives more than 4

219   times the solubility enhancement of any other organic acid. The superior performance of caffeic acid may

220   be due to disruption of metal bridges between SOM segments owing to its chelation ability (via *ortho*

221   hydroxyl groups), which is exclusive to caffeic acid among the organic acids tested.

222   The normalized solubility—that is, the ratio of solubility in organic acid solution to the solubility

223   in the respective NaCl/water control solution from the data of Figure 4—is shown in Figure 5.

224   Normalized solubility increases with organic acid concentration in the examples where comparisons were

225   made (formic, benzoic, and 4-hydroxybenzoic). Normalized solubility trends weakly with organic acid

226   molecular weight (R^2: 0.554 for 1 M; 0.072 for 0.3 M; and 0.631 for 0.1 M organic acid). The trend with

227   molecular weight may be due to a contribution by van der Waals interactions between the displacing

228   organic acid molecule and the SOM segments that helps drive solubilization (see Scheme 1a).

3.2. Column studies

229

230   Figure 6 shows the results of experiments in which a column of Pahokee peat particles dispersed

231 in glass microbeads was eluted with 2 M acetate, formate, or NaCl solution as control. The column was

232 conditioned with 2 M NaCl at pH 5.3 before switching the influent to the 2 M organic acid solution

233 adjusted to the same pH and ionic strength. About 100 min after the influent was switched, the

234 absorbance abruptly increased from about 2 to about 10 units for formate, and from about 2 to about 5

235 units for acetate over a 50 min period, and then declined toward the original value. At the same time, the

236 pH increased from 5.32 to 5.44 for formate, or from 5.24 to 5.39 for acetate. A blank column in which

237 Pahokee peat was ommitted from the packing material showed no changes in solution absorbance or pH

238 upon switching the eluent to formate (bottom panel in Figure 6).

239   The column experiments confirm the results of the batch experiments that organic acids displace

240 OM into solution. Consistent with disruption of (-)CAHBs is the greater release of DOM in the case of

241 formate than acetate. The results further show that displacement of OM into solution occurs

242 coincidentally with uptake of protons from the solution (release of hydroxide to solution). We ascribe

243 proton uptake to the formation of (-)CAHB between free carboxylate groups on OM and formate or

244 acetate ions, according to the reaction shown in Scheme 1b based on eq 1. Quantification of proton uptake

245 is made complicated by the buffering capacity of SOM and the organic acid itself, as well as possibly the

246 rates of proton exchange with the liquid phase.

4. CONCLUSIONS AND IMPLICATIONS

247

248   The results of this study provide insight into the molecular-level associations that OM can engage

249 with geosolids. The CAHB makes OM molecules "stickier" (more cohesive and adhesive), affecting

250 solubility, molecular aggregation in solution, and adsorption to mineral and biological surfaces.

251 Formation of CAHBs may contribute to supramolecular aggregation of DOM, which can influence the

252 transport of DOM in the vadose and saturated zones. Some evidence in support of the contribution of

11

253   (-)CAHB to supramolecular aggregation already exists, although not recognized by the researchers: the

254   finding that diazomethane treatment promotes disaggregation of DOM[14]; and the finding that simple

255   carboxylic acids break up OM supra-aggregates more readily than methanol [8]. Plant root exudates are

256   commonly aromatic acids; these exudates may help mobilize SOM in the rhizosphere via CAHB, which,

257   in turn, may impact adsorption, solubility, and bioavailability of OM. The pK_a of the (-)CAHB complex is

258   1-3 units above those of the free acids [17]; therefore, such bonds may influence the buffering capacity of

259   OM. Lastly, it is possible that (-)CAHBs may compete with transition metal ion coordination to carboxyl

260   sites on DOM, based on the results for Cu^{2+} complexation with simple organic acids in solution [40].

261   The potential of OM to form (-)CAHB also has implications with respect to its interactions with

262   anthropogenic substances. Already mentioned in the Introduction is the known role that (-)CAHB plays in

263   interactions of small weak acids (contaminants of concern and others) with the surfaces of chars and

264   partially-oxidized carbon nanotubes. Other situations in which (-)CAHB can be of importance are the

265   interactions between DOM and chars, which are ubiquitous in soil and sediment; between DOM and

266   carbon nanotubes; and between DOM and other engineered nanomaterials functionalized with coatings

267   that have weak acid groups. For example, citrate groups on citrate-coated gold nanoparticles (CIT-nAu),

268   render the particles sticky under certain conditions towards each other [41] and to black carbon (biochar)

269   surfaces through interactions between carboxyl groups on opposing entities.[42] Esfahani et al.[43] [44] found

270   that CT-nAu promotes disaggregation of DOM and becomes "overcoated" by OM, possibly through

271   (-)CAHB interactions between bound citrate and OM carboxyl groups.

272

1
2
3
4
5
6
7
8
9
10
11
12
13
14
15
16
17
18
19
20
21
22
23
24
25
26
27
28
29
30
31
32
33
34
35
36
37
38
39
40
41
42
43
44
45
46
47
48
49
50
51
52
53
54
55
56
57
58
59
60

277 **REFERENCES**

278 1. R. S. Swift, Macromolecular properties of soil humic substances: Fact, fiction, and opinion., *Soil*
279 *Sci.* , 1999, **164**, 790-802.
280 2. R. S. Cameron, B. K. Thornton, R. S. Swift and A. M. Posner, Molecular weight and shape of
281 humic acid from sedimentation and diffusion measurements on fractionated extracts., *J. Soil*
282 *Sci.*, 1972, **23**, 394-408.
283 3. M. M. Kononova, *Soil organic matter, its nature, its role in soil formation and in soil fertility.* ,
284 Pergamon Press, New York, NY, 1961.
285 4. F. Stevenson, *Humus chemistry: Genesis, Composition, Reactions*, Wiley, New York, NY, 2nd edn.,
286 1994.
287 5. A. Piccolo, in *Adv. Agron.*, Elsevier, 2002, vol. 75, pp. 57-134.
288 6. A. Piccolo, S. Nardi and G. Concheri, Macromolecular changes of humic substances induced by
289 interaction with organic acids., *Eur. J. Soil Sci.*, 1996, **47**, 319-328.
290 7. A. Piccolo, S. Nardi and G. Concheri, Micelle-1ike conformation of humic substances as revealed
291 by size exclusion chromatography. , *Chemosphere*, 1996, **33**, 595-602.
292 8. P. Conte and A. Piccolo, Conformational arrangement of dissolved himic substances. influence of
293 solution composition on association of humic molecules, *Environ. Sci. Technol*, 1999, **33**, 1682-
294 1690.
295 9. A. Piccolo, The supramolecular structure of humic substances: a novel understanding of humus
296 chemistry and implications in soil science, *Adv. Agron.*, 2001, **75**, 699 -706.
297 10. D. Smejkalova and A. Piccolo, Aggregation and disaggregation of humic supramolecular
298 assemblies by NMR diffusion ordered spectroscopy (DOSY-NMR), *Environ. Sci. Technol.*, 2008,
299 **42**, 699-706.
300 11. R. Sutton and G. Sposito, Molecular Structure in Soil Humic Substances: The New View;
301 doi:10.1021/es050778q, *Environ. Sci. Technol.*, 2005, **39**, 9009-9015.
302 12. A. J. Simpson, Determining the molecular weight, aggregation, structures and interactions of
303 natural organic matter using diffusion ordered spectroscopy., *Magnet. Reson. Chem.*, 2002, **40**,
304 S72-S82.
305 13. A. C. Stenson, W. M. Landing, A. G. Marshall and W. T. Cooper, Ionization and fragmentation of
306 humic substances in electrospray ionization Fourier transform-ion cyclotron resonance mass
307 spectrometry, *Anal. Chem.*, 2002, **74**, 4397-4409.
308 14. C. E. Rostad and J. A. Leenheer, Factors that affect molecular weight distribution of Suwannee
309 river fulvic acid as determined by electrospray ionization/mass spectrometry, *Anal. Chim. Acta*,
310 2004, **523**, 269-278.
311 15. D. Petrov, D. Tunega, M. H. Gerzabek and C. Oostenbrink, Molecular Dynamics Simulations of
312 the Standard Leonardite Humic Acid: Microscopic Analysis of the Structure and Dynamics,
313 *Environ. Sci. Technol.*, 2017, **51**, 5414-5424.
314 16. R. Sutton, G. Sposito, M. S. Diallo and H. R. Schulten, Molecular simulation of a model of
315 dissolved organic matter, *Environ. Toxicol. Chem.*, 2005, **24**, 1902-1911.
316 17. X. Li, J. J. Pignatello, Y. Wang and B. Xing, New Insight into the Mechanism of Adsorption of
317 Ionizable Compounds on Carbon Nanotubes *Environ. Sci. Technol.*, 2013, **47**, 8334-8341.
318 18. W. W. Cleland, Low-Barrier Hydrogen-Bonds and Low Fractionation Factor Bases in Enzymatic-
319 Reactions, *Biochem.*, 1992, **31**, 317-319.
320 19. G. Gilli and P. Gilli, *The Nature of the Hydrogen Bond: Outline of a Comprehensive Hydrogen*
321 *Bond Theory*, Oxford University Press, 2009.

322   20.   G. Gilli and P. Gilli, Towards an unified hydrogen-bond theory, *J. Molec. Structure*, 2000, **552**, 1-
323   15.
324   21.   P. Gilli, L. Pretto, V. Bertolasi and G. Gilli, Predicting Hydrogen-Bond Strengths from Acid-Base
325   Molecular Properties. The pK(a) Slide Rule: Toward the Solution of a Long-Lasting Problem, *Acc.*
326   *Chem. Res.*, 2009, **42**, 33-44.
327   22.   P. Schah-Mohammedi, I. G. Shenderovich, C. Detering, H.-H. Limbach, P. M. Tolstoy, S. N.
328   Smirnov, G. S. Denisov and N. S. Golubev, Hydrogen/Deuterium-Isotope Effects on NMR
329   Chemical Shifts and Symmetry of Homoconjugated Hydrogen-Bonded Ions in Polar Solution, *J.*
330   *Am. Chem. Soc*, 2000, **122**, 12878-12879.
331   23.   P. M. Tolstoy, P. Schah-Mohammedi, S. N. Smirnov, N. S. Golubev, G. S. Denisov and H. H.
332   Limbach, Characterization of fluxional hydrogen-bonded complexes of acetic acid and acetate by
333   NMR: Geometries and isotope and solvent effects, *J. Am. Chem. Soc*, 2004, **126**, 5621-5634.
334   24.   W. W. Cleland and M. M. Kreevoy, Low-barrier hydrogen bonds and enzymic catalysis, *Science*,
335   1994, **264**, 1887-1890.
336   25.   M. D. Ward, in *Molecular Networks*, ed. M. W. Hosseini, 2009, vol. 132, pp. 1-23.
337   26.   D. Braga and F. Crepioni, Intermolecular interactions in nonorganic crystal engineering, *Acc.*
338   *Chem. Res.*, 2000, **33**, 601-608.
339   27.   J. Ni, J. J. Pignatello and B. Xing, Adsorption of Aromatic Carboxylate Ions to Charcoal Black
340   Carbon is Accompanied by Proton Exchange with Water,, *Environ. Sci. Technol.*, 2011, **45**, 9240-
341   9248.
342   28.   M. Teixido, J. J. Pignatello, J. L. Beltran, M. Grenados and J. Peccia, Speciation of the Ionizable
343   Antibiotic Sulfamethazine on Black Carbon (Biochar), *Environ. Sci. Technol.*, 2011, **45**, 10020-
344   10027.
345   29.   X. Li, B. Gamiz, Y. Wang, J. J. Pignatello and B. Xing, Competitive Sorption Used to Probe Strong
346   Hydrogen Bonding Sites for Weak Organic Acids on Carbon Nanotubes, *Environ. Sci. Technol.*,
347   2015, **49**, 1409-1417.
348   30.   F. Xiao and J. J. Pignatello, Effects of Post-Pyrolysis Air Oxidation of Biomass Chars on Adsorption
349   of Neutral and Ionizable Compounds, *Environ. Sci. Technol.*, 2016, **50**, 6276-6283.
350   31.   R. Baziramakenga, R. R. Simard and G. D. Leroux, Determination of organic-acids in soil extracts
351   by ion chromatography, *Soil Biol. Biochem.*, 1995, **27**, 349-356.
352   32.   S. Deiana, C. Gessa, M. Marchetti and M. Usai, Phenolic-Acid Redox Properties - Ph Influence on
353   Iron(Iii) Reduction by Caffeic Acid, *Soil Sci. Soc. Am. J.*, 1995, **59**, 1301-1307.
354   33.   B. Klejdus and V. Kuban, Plant phenolic compounds in allelopathy, *Chemicke Listy*, 1999, **93**, 243-
355   248.
356   34.   C. Bertin, X. H. Yang and L. A. Weston, The role of root exudates and allelochemicals in the
357   rhizosphere, *Plant and Soil*, 2003, **256**, 67-83.
358   35.   J. O. Siqueira, M. G. Nair, R. Hammerschmidt and G. R. Safir, Significance of Phenolic-
359   Compounds in Plant-Soil-Microbial Systems, *Critical Reviews in Plant Sciences*, 1991, **10**, 63-121.
360   36.   J. D. Ritchie and E. M. Perdue, Proton-binding study of standard and reference fulvic acids,
361   humic acids, and natural organic matter, *Geochim. Cosmochim. Acta*, 2003, **67**, 85-96.
362   37.   B. Xing and J. J. Pignatello, Dual-mode sorption of low-polarity compounds in glassy poly(vinyl
363   chloride) and soil organic matter, *Environ. Sci. Technol*, 1997, **31**, 792-799.
364   38.   M. Y. Z. Abouleish and M. J. M. Wells, Trihalomethane formation potential of aquatic and
365   terrestrial fulvic and humic acids: Sorption on activated carbon, *Sci. Tot. Environ.*, 2015, **521-522**,
366   293-304.
367   39.   M. Meot-Ner (Mautner) and L. W. Sieck, The ionic hydrogen bond and ion solvation. 5. OH...O-
368   bonds. Gas-phase solvation and clustering of alkoxide and carboxylate anions, *J. Am. Chem. Soc*,
369   1986, **108**, 7525-7529.

14

370 40. J. Zhao, G. Chu, B. Pan, Y. Zhou, M. Wu, Y. Liu, W. Duan, D. Lang, Q. Zhao and B. Xing, Homo-
371   Conjugation of Low Molecular Weight Organic Acids Competes with Their Complexation with
372   Cu(II), *Environ. Sci. Technol.*, 2018, **52**, 5173-5181.
373 41. J. W. Park and J. S. Shumaker-Parry, Structural study of citrate layers on gold nanoparticles: Role
374   of intermolecular interactions in stabilizing nanoparticles., *J. Am. Chem. Soc.*, 2014, **136**, 1907-
375   1921.
376 42. M. Uchimiya, J. J. Pignatello, J. C. White, S.-L. Hu and P. J. Ferreira, Surface Interactions between
377   Gold Nanoparticles and Biochar, *Sci Rep-Uk*, 2017, **7**, 5027.
378 43. M. R. Esfahani, V. L. Pallem, H. A. Stetz and M. J. M. Wells, Humic acid disaggregation with/of
379   gold nanoparticles: effects of nanoparticle size and pH, *Environmental Nanotechnology,*
380   *Monitoring & Management*, 2016, **6**, 54-63.
381 44. M. R. Esfahani, V. L. Pallem, H. A. Stretz and M. J. M. Wells, Core-size regulated
382   aggregation/disaggregation of citrate-coated gold nanoparticles (5–50nm) and dissolved organic
383   matter: Extinction, emission, and scattering evidence, *Spectrochimica Acta Part A: Molecular*
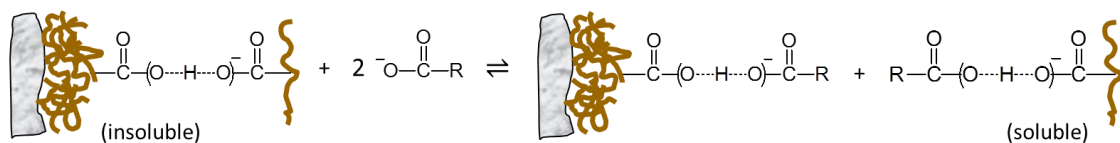384   *and Biomolecular Spectroscopy*, 2018, **189**, 415-426.

385

386

387
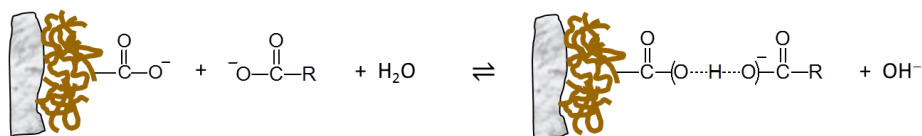
1
2
3
4
5
6
7
8
9
10
11
12
13
14
15
16
17
18
19
20
21
22
23
24
25
26
27
28
29
30
31
32
33
34
35
36
37
38
39
40
41
42
43
44
45
46
47
48
49
50
51
52
53
54
55
56
57
58
59
60

388

a) Enhancement of water solubility:

(insoluble)   + 2 $^-$O–C–R ⇌   + R–C–(O···H···O)–C (soluble)

b) Release of hydroxide ion:

–C–O$^-$ + $^-$O–C–R + H_2O ⇌ –C–(O···H···O)–C–R + OH^-

c) Facilitation of supramolecular aggregate dispersion:

RCO_2H/RCO_2^- ⇌

389

390   **Scheme 1.** Hypothesized CAHB interactions of carboxylate ions with OM: a) disruption of OM-OM
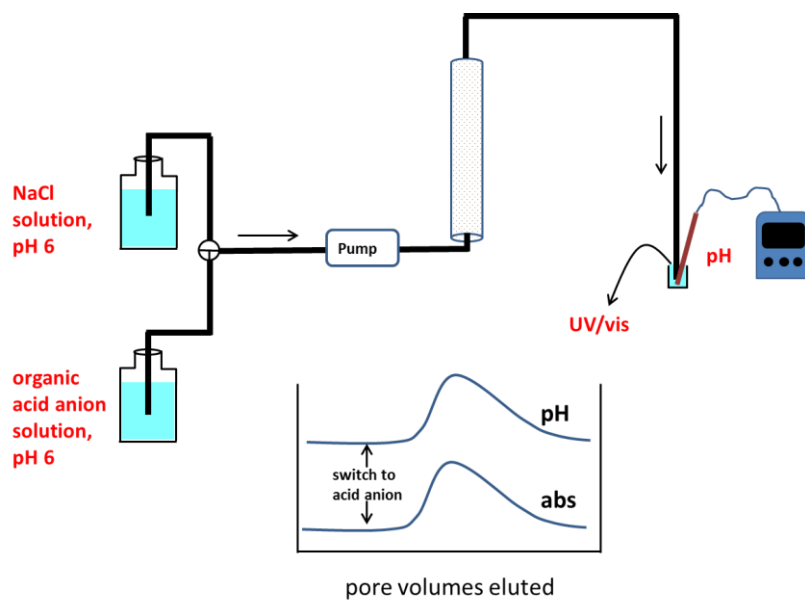
391   CAHBs in OM anchored to a particle (gray shape) resulting in partial solubilization; b) formation of new

392   OM-carboxylate CAHBs leading to release of hydroxide ions into solution; and c) disruption of OM-OM

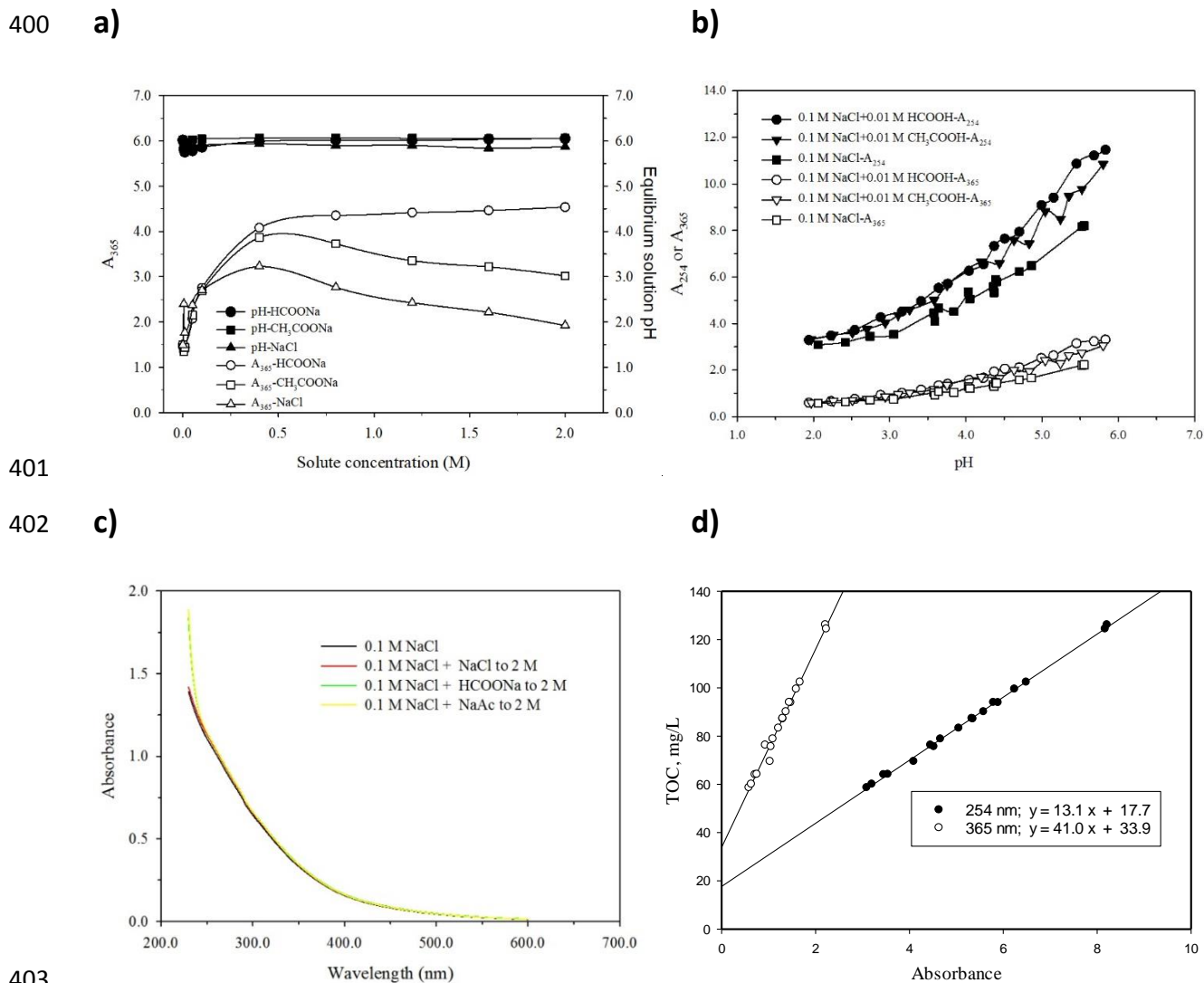393   interactions within supramolecular aggregates leading to their dispersion.

394

395

396

397   **Figure 1.** Scheme of column elution experiment. After a time, the eluent is switched from the NaCl
398   solution to the organic acid anion solution at the same ionic strength. The pH and absorbance of the
399   effluent was monitored.

400 **a)**

b)

401

402 **c)**

d)

403
404
405

406 **Figure 2.** Use of absorbance as surrogate for DOM concentration. **a)** Absorbance at 365 nm of DOM

407 extracted by different solutions in the undiluted supernatant at pH 6 is dependent on salt composition and

408 concentration. **b)** Absorbance ratio A_{254}/A_{365} in the undiluted supernatant is pH-dependent. **c)** Absorbance

409 spectrum of a DOM solution of different compositions after 10-fold dilution into phosphate buffer at pH

410 6.5 showing the spectrum is no longer sensitive to initial sample composition and pH. **d)** Correlation

411 between absorbance and total non-purgeable total organic carbon content of water extracts of Pahokee

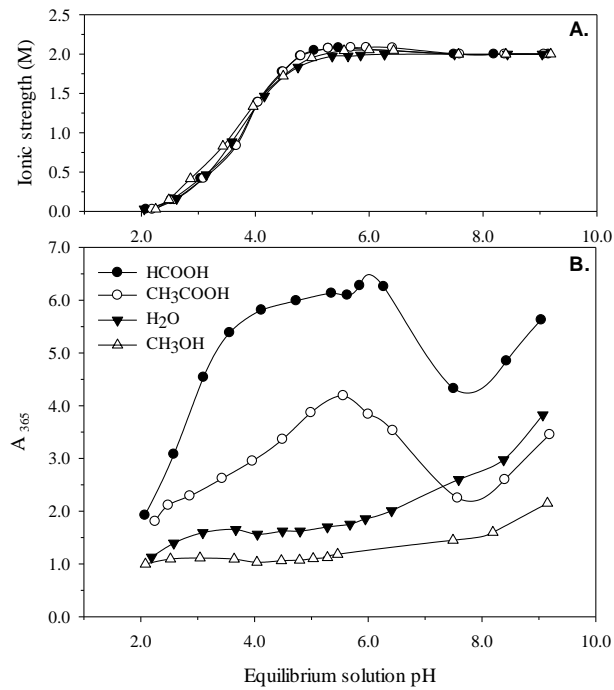412 peat obtained at different pH and uniform ionic strength of 0.1 M. The TOC was measured directly and

413   the absorbance was measured after dilution into the pH 6.5 phosphate buffer and then corrected for
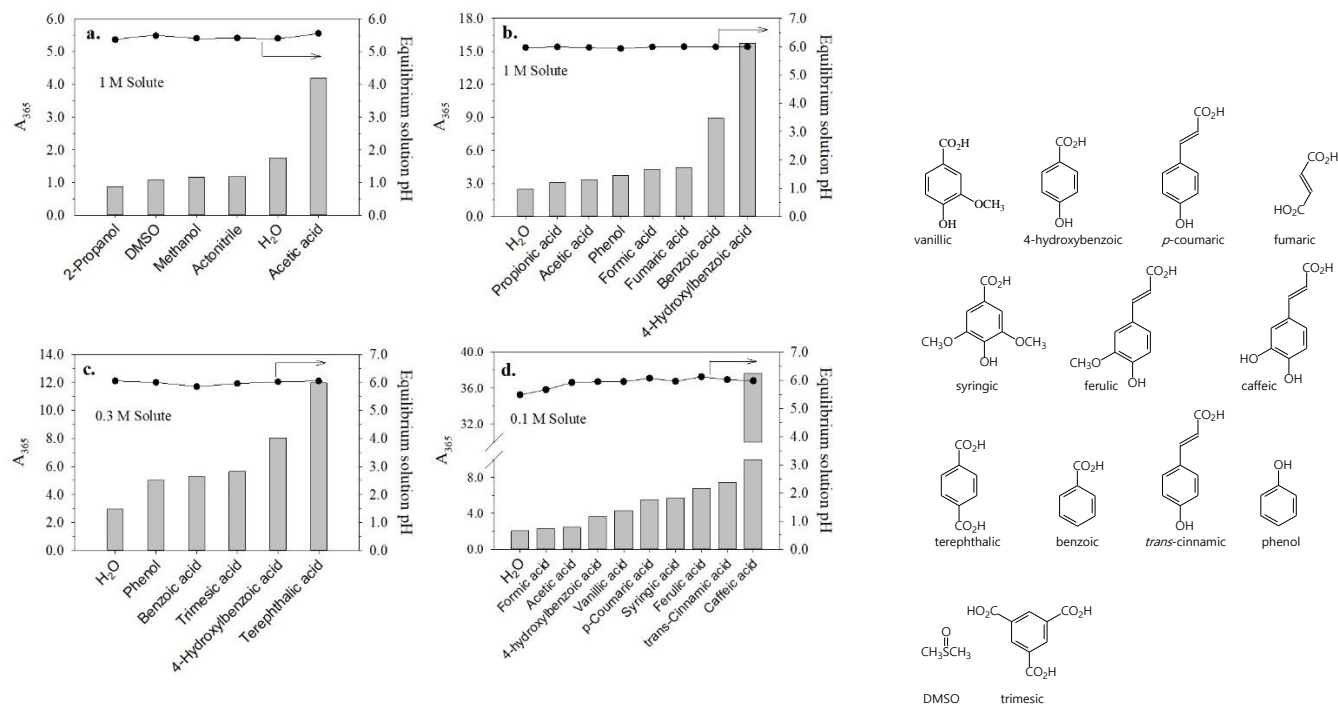
414   dilution.

415

416

417

Figure 3. A) Absorbance at 365 nm of DOM extracted by different solutions (2 M formic acid, acetic

acid, methanol, or NaCl) as a function of pH. B) Adjusted ionic strength calculated at each measured pH

in each experiment in Panel A.

421

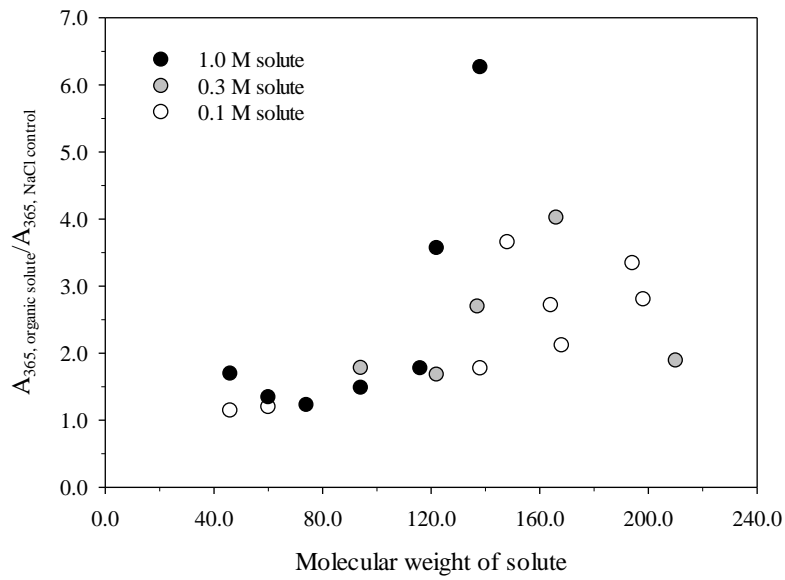1
2
3
4
5
6
7
8
9
10
11
12
13
14
15
16
17
18
19
20
21
22
23
24
25
26

422

27
28
29
30
31
32

Figure 4. Twenty-four hour solubility of organic matter from Pahokee peat in water containing different

organic solutes or NaCl (control) at the specified concentration (in panel **b**, phenol is 0.8 M due to

solubility limitation).

33
34
35
36
37
38
39
40
41
42
43
44
45
46
47
48
49
50
51
52
53
54
55
56
57
58
59
60

423

424

425

426

21

1
2
3
4
5
6
7
8
9
10
11
12
13
14
15
16
17
18
19
20
21
22
23
24
25
26
27
28
29
30
31
32
33
34
35
36
37
38
39
40
41
42
43
44
45
46
47
48
49
50
51
52
53
54
55
56
57
58
59
60

427

Figure 5. Solubility of Pahokee OM in aqueous solutions of organic acids at different concentrations

(data from Figure 6) normalized to the NaCl control as a function of organic acid molecular weight.
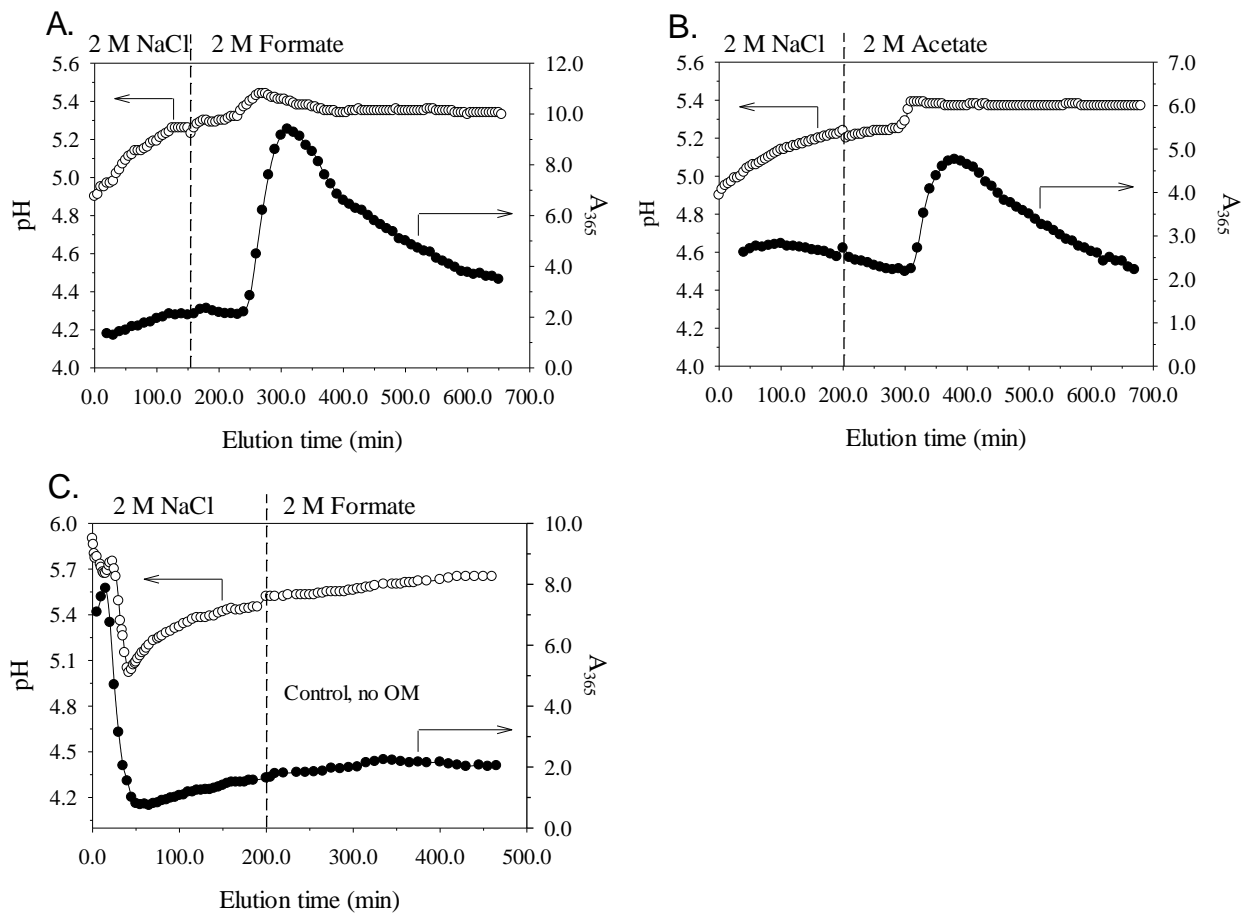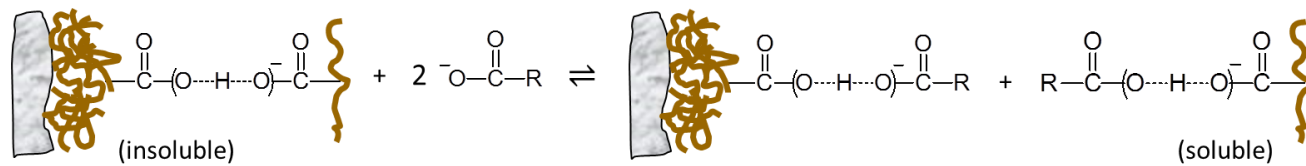
430

Figure 6. Column experiments with Pahokee peat dispersed in glass microbeads and eluted with 2 M

NaCl, then switched to formate (A and C) or acetate (B). Panel C represents the control column, which

contained only glass microbeads and no peat.

23

442   GRAPHICAL ABSTRACT

443

444

445   Solubility experiments suggest that very strong hydrogen bonds between weak acid functional groups
446   play an important role in organic matter cohesion.

447